4. A. D. Del Genio and W. B. Rossow, *J. Atmos. Sci.* **47**, 293 (1990).
5. W. B. Rossow, A. D. Del Genio, T. P. Eichler, *ibid.*, p. 2053.
6. M. Marov *et al.*, *ibid.* **30**, 1210 (1973).
7. V. V. Kerzhanovich and M. Ya. Marov, in *Venus*, D. M. Hunten, L. Colin, T. M. Donahue, V. I. Moroz, Eds. (Univ. of Arizona Press, Tucson, 1983), pp. 776–778.
8. C. C. Counselman III, S. A. Gourevitch, R. W. King, G. B. Loriot, R. G. Prinn, *Science* **205**, 85 (1979).
9. J. E. Blamont *et al.*, *ibid.* **231**, 1422 (1986).
10. R. A. Preston *et al.*, *ibid.*, p. 1414.
11. M. J. S. Belton *et al.*, *ibid.* **253**, 1531 (1991).
12. D. Crisp *et al.*, *ibid.*, p. 1538.
13. R. W. Carlson *et al.*, *ibid.*, p. 1541.
14. G. Schubert, in (*7*), pp. 681–765.
15. V. S. Avduevsky *et al.*, *Cosmic Res.* **14**, 622 (1976).
16. R. Greeley *et al.*, *Icarus* **57**, 112 (1984).
17. E. Kálnay de Rivas, *J. Atmos. Sci.* **30**, 763 (1973).
18. P. H. Stone, *ibid.* **31**, 1681 (1974).
19. G. Schubert *et al.*, *J. Geophys. Res.* **85**, 8007 (1980).
20. W. B. Rossow, *J. Atmos. Sci.* **40**, 273 (1983).
21. ———, *Adv. Geophys.* **28A**, 347 (1985).
22. R. S. Saunders *et al.*, *Science* **252**, 249 (1991).
23. R. Greeley *et al.*, *J. Geophys. Res.* **97**, 13319 (1992).
24. R. E. Arvidson *et al.*, *ibid.*, p. 13303.
25. C. A. Sagan *et al.*, *Icarus* **17**, 346 (1972).
26. P. Thomas, J. Veverka, S. Lee, A. Bloom, *ibid.* **45**, 124 (1981).
27. R. Greeley, P. Christensen, R. Carrasco, *Geology* **17**, 665 (1989).
28. R. Greeley, J. D. Iversen, J. B. Pollack, N. Udovich, B. White, *Science* **183**, 847 (1974).
29. R. S. Saunders, A. R. Dobrovolskis, R. Greeley, S. D. Wall, *Geophys. Res. Lett.* **17**, 1365 (1990).
30. P. Thomas and J. Veverka, *J. Geophys. Res.* **84**, 8131 (1979).
31. P. H. Schultz, *ibid.* **97**, 16183 (1992).
32. D. B. Campbell *et al.*, *ibid.*, p. 16249.
33. We thank R. D. Baker and D. L. Bindschadler for helpful discussions and E. Lo for developing programs to manipulate the database. Supported by the National Aeronautics and Space Administration through the Magellan Project and the Office of Planetary Geoscience.

17 August 1993; accepted 18 November 1993

500,000-Year Stable Carbon Isotopic Record from Devils Hole, Nevada

Tyler B. Coplen,* Isaac J. Winograd, Jurate M. Landwehr, Alan C. Riggs

The record of carbon-13 ($\delta^{13}C$) variations in DH-11 vein calcite core from Devils Hole, Nevada, shows four prominent minima near glacial terminations (glacial-interglacial transitions) V to II. The $\delta^{13}C$ time series is inversely correlated with the DH-11 oxygen isotope ratio time series and leads it by as much as 7000 years. The $\delta^{13}C$ variations likely record fluctuations in the $\delta^{13}C$ of dissolved inorganic carbon of water recharging the aquifer. How such variations are transported 80 kilometers to Devils Hole without obliteration by water-rock reaction remains an enigma. The record may reflect (i) global variations in the $\delta^{13}C$ of atmospheric CO_2 and, hence, the $\delta^{13}C$ of continental biomass or (ii) variations in extent and density of vegetation in the southern Great Basin. In the latter case, $\delta^{13}C$ minima at 414, 334, 246, and 133 thousand years ago mark times of maximum vegetation.

We have obtained a detailed and well-dated record of $\delta^{13}C$ variations in southern Great Basin ground waters for the period 60 to 566 thousand years ago (ka) from vein-calcite core DH-11 (*1–3*) from Devils Hole at the distal end of the Ash Meadows ground-water basin, Nevada (Fig. 1). This basin has an area greater than 12,000 km^2 and comprises a thick section (~100 to >1000 m) of Paleozoic carbonate rocks that transmit water chiefly through fractures (*4*). The Spring Mountains, Pahranagat Valley, and possibly the Sheep Range (Fig. 1) are the principal recharge areas (*4, 5*). Recharge also occurs by downward leakage from Tertiary volcanic and lacustrine aquitards (*4*). Devils Hole is near the center of the principal discharge area, a 16-km-long, fault-controlled spring lineament at Ash Meadows (Fig. 1).

Vein-calcite samples from four locations in Devils Hole displayed $\delta^{13}C$ and $\delta^{18}O$ profiles versus time that are nearly identical (*6*). Our longest record, DH-11, is based on analysis of 285 samples (*2*) and shows periods of as much as tens of thousands of years during which the $\delta^{13}C$ of precipitating calcite was relatively constant (−1.6 to −1.8 per mil). These periods are separated by four prominent $\delta^{13}C$ troughs approximately centered on glacial terminations V through II, as delineated by the DH-11 $\delta^{18}O$ record (Fig. 2). In general (especially near terminations V to III), the $\delta^{13}C$ curve begins to decline at about the time the $\delta^{18}O$ curve reaches its minimum (glacial maximum). The $\delta^{13}C$ curve subsequently reaches its lowest (most negative) values at about the time that the $\delta^{18}O$ curve peaks (maximum interglacial conditions). Then, the $\delta^{13}C$ curve rapidly reverses direction (increasing $^{13}C/^{12}C$ ratio), whereas the $\delta^{18}O$ curve remains relatively high (at peak interglacial values) for 10,000 to 20,000 years before declining (*7*).

Although arising from distinct and independent geochemical processes, the DH-11 $\delta^{13}C$ profile (Fig. 2) is highly correlated ($r = -0.75$ with a $\delta^{18}O$ lag of 7000 years; Fig. 3) with the $\delta^{18}O$ time series (*8*). Spectral analyses (*8*) indicate robust peaks (in order of decreasing power) of 93,000, 40,000, 25,000, 23,000, and 17,000 years for the $\delta^{18}O$ time series and of 91,000, 40,000, 23,000, 28,000 and 18,000 years for the $\delta^{13}C$ data. Thus, obliquity and precession periodicities are evident in the DH-11 $\delta^{13}C$ record.

^{14}C and ^{13}C concentrations in dissolved inorganic carbon (DIC) from points along the flow path of the modern Ash Meadows ground-water basin indicate that extensive carbon exchange between water and aquifer rock occurs in the aquifer (*9, 10*). For example, ^{14}C and ^{13}C content vary from 79 pmc (percent modern carbon) and −9.5 per mil, respectively, in the Spring Mountains recharge waters, to 8.43 pmc and −7.6 per mil at Indian Springs (Fig. 1), 18 km down the hydraulic gradient. Ground water reaching Ash Meadows, tens of kilometers from Indian Springs, has average ^{14}C and $\delta^{13}C$ values of 2.1 pmc and −4.8 per mil, respectively (*5*). This carbon exchange is probably driven by episodes of calcite dissolution and precipitation as the ground-water flow alternates from depths of hundreds to more than a thousand meters below land surface and as temperature increases from 8° to 34°C (*5*). Carbon-isotope buffering tends to drive ^{13}C content of DIC toward equilibrium with aquifer carbonate rocks, which have $\delta^{13}C$ values ranging from ~−2 per mil (*11*) to perhaps several per mil more positive. This buffering also decreases the ^{14}C content of DIC, and ^{14}C ages are thousands of years too old (*2*).

With evidence for such extensive buffering, we expected to find a relatively featureless $\delta^{13}C$ profile in DH-11 calcite, not the impressive range and detail of the $\delta^{13}C$ fluctuations and the correlation with the $\delta^{18}O$ time series [which is assumed to be conservative in a low-temperature (<35°C) carbonate-rock aquifer]. In standard deviation units, many of the major $\delta^{13}C$ variations are larger than those of $\delta^{18}O$ (Fig. 3). That the DH-11 $\delta^{13}C$ record is responding in a significant manner to global climate is strongly suggested by these relations (Fig. 3).

We are unable to identify any process within the ground-water flow system that could generate the DH-11 $\delta^{13}C$ variations. We rule out several aquifer specific and general factors including (i) variation in water temperature or water level in Devils

T. B. Coplen, I. J. Winograd, J. M. Landwehr, U.S. Geological Survey, 431 National Center, Reston, VA 22092.
A. C. Riggs, U.S. Geological Survey, Denver Federal Center, MS 421, Lakewood, CO 80225.
*To whom correspondence should be addressed.

Hole (*12*), (ii) precipitation of calcite in isotopic disequilibrium (*13*), (iii) fluctuation in ground-water pH (*14*), (iv) occasional input of surface water to Devils Hole during storms (*15*), (v) variations in the fractions of flow derived from the principal recharge areas (*16*), (vi) varying ground-water residence times (*17, 18*), and (vii) varying growth rate of the vein calcite (*19*). We conclude that variations in the $\delta^{13}C$ profile must occur before carbon enters the aquifer.

How such variations are transmitted (albeit shifted to increasing $\delta^{13}C$ values) through the aquifer to Devils Hole >80 km distant without obliteration remains a major geochemical enigma. Nevertheless, we tentatively assume that the amount of buffering of each packet of water transversing the aquifer in the past was approximately constant in order for source variations to be transmitted.

Source variations of $\delta^{13}C$ may result from (i) variations in the relative abundance of plants in the principal recharge areas using C3 and C4 photosynthetic pathways; (ii) varying partial pressure of atmospheric CO_2 (pCO_2), which may affect the $\delta^{13}C$ of soil CO_2 and hence of DIC; (iii) varying $\delta^{13}C$ of atmospheric CO_2 and, hence, the $\delta^{13}C$ of continental biomass; and (iv) varying density and areal distribution of vegetation. Of these, the first does not seem to be important in the Ash Meadows system (*20, 21*). We also eliminate global pCO_2 variations because $\delta^{13}C$ values in DH-11 shift abruptly during peak interglacial times [133 to 118 ka (Fig. 2)] when atmospheric pCO_2 [derived from the Vostok ice core (*22*)] remained relatively constant.

Prominent $\delta^{13}C$ troughs centered approximately on terminations, as for DH-11 (Fig. 2), are also present in numerous $\delta^{13}C$ records of plankton in marine cores (*23–26*), including cores from regions with no upwelling where oceanic DIC might approach carbon isotopic equilibrium with atmospheric CO_2 (*23, 24, 27*) (Fig. 4). These marine $\delta^{13}C$ records (Fig. 4) also resemble the DH-11 curve in that the minima occur as much as several thousand years before $\delta^{18}O$ interglacial peaks [see (*24*)]. In both the marine and Devils Hole records, the descent from more positive $\delta^{13}C$ values begins as much as 20,000 years before the terminations, and the trough near termination III is not as distinct as those near terminations V, IV, and II. However, the amplitude of the $\delta^{13}C$ minimum centered on termination II is generally <1 per mil in the planktonic records (*23, 24, 26*) versus 1.3 per mil in DH-11. Moreover, because of reactions of water with Paleozoic carbonate detritus [$\delta^{13}C$ of −1 per mil (*11*)] in the soil, a 1.3 per mil change in the $\delta^{13}C$ of the DH-11 core would (for closed system conditions) require a change in the $\delta^{13}C$ of atmospheric CO_2 of ~2.6 per mil. The largest shift in a marine record is 2.1 per mil (*23*), although bioturbation could have reduced the signal in some records (*24*).

Is there any evidence for an atmospheric $\delta^{13}C$ teleconnection between the marine and DH-11 records? Krishnamurthy and Epstein (*28*) reported that $\delta^{13}C$ values in wood cellulose decreased by 4 per mil across termination I. They attributed this decline to a change in the $\delta^{13}C$ of atmospheric

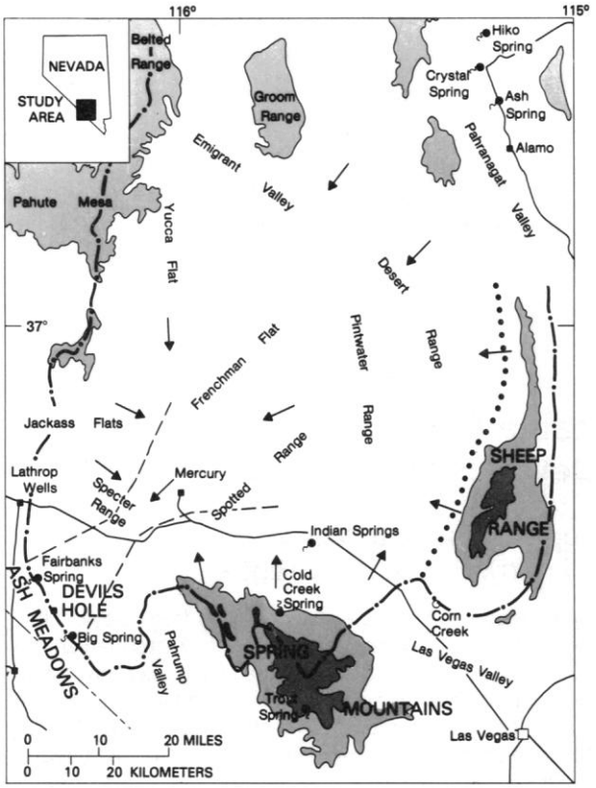

Fig. 1. Index map of southcentral Great Basin, modified after (*3*). Major mountains are shaded: heavy shading denotes altitudes of 2400 to 3600 m above sea level; light shading denotes altitudes of 1800 to 2400 m above sea level; ridge tops <1800 m above sea level are designated by name only. Heavy dashed and dotted line is the boundary of Ash Meadows ground-water basin (*4*); heavy dotted line is alternate eastern boundary (*2*). Arrows denote general direction of ground-water flow in aquifer as inferred from potentiometric maps (*4*). Dashed line is a major trough in potentiometric surface of carbonate aquifer. Solid line connecting Las Vegas and Lathrop Wells is U.S. Highway 95.

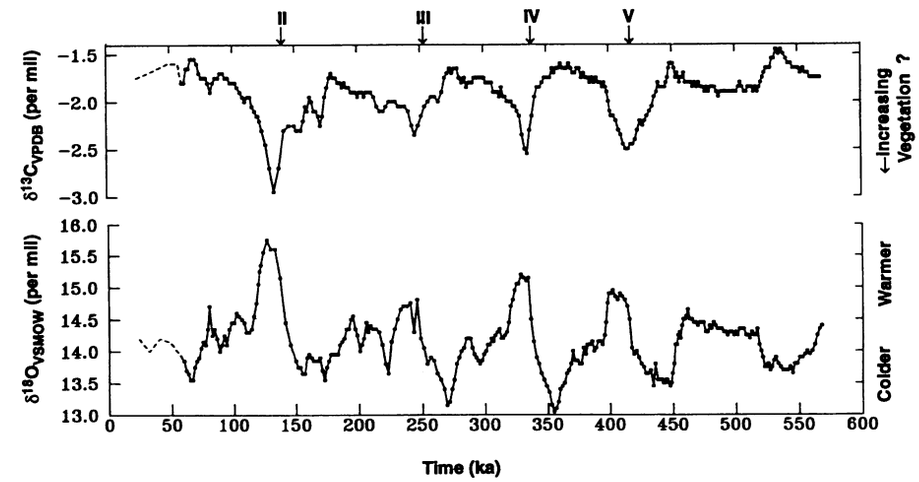

Fig. 2. Variations in $\delta^{13}C$ and $\delta^{18}O$ in core DH-11 during middle and late Pleistocene. Each dot represents an analysis; ages were assigned by interpolation between ^{230}Th-^{234}U-^{238}U dated sections of core (*1, 2*). Ages are minimum ages and need to be increased by ground-water travel times, which may be several thousands of years (*2*). Roman numerals denote approximate timing of glacial terminations (glacial-interglacial transitions) as in (*2*). Carbon isotope ratios are in per mil relative to VPDB [Vienna Peedee belemnite, defined by $\delta^{13}C_{NBS19/VPDB} \equiv +1.95$ per mil (*42*)]. Oxygen isotope results are in per mil relative to VSMOW (Vienna Standard Mean Ocean Water) on a scale normalized such that SLAP (Standard Light Antarctic Precipitation) is −55.5 per mil (*42*). The $\delta^{13}C$ and $\delta^{18}O$ 1-σ analytic errors are 0.05 and 0.07 per mil, respectively. Dashed lines are based on analysis of five samples spanning the interval 57 to 24 ka of vein calcite sample DH-7 (*6*).

CO_2, which in turn is believed to reflect changes in ocean productivity. Marino *et al.* (*29*) analyzed the cellulose of plants from southern Nevada packrat middens, specifically the C4 plant *Altriplex confertifolia*, known to record accurately $\delta^{13}C$ variations of atmospheric CO_2 when not under salt stress. Their data display a prominent $\delta^{13}C$ minimum of ~1.1 per mil; however, the minimum is at ~18 ka, several thousand years before termination I. In contrast, analysis of the Byrd ice core (*30*) suggests that atmospheric $\delta^{13}C$ shifted only 0.3 per mil across termination I, and full glacial values were more negative than Holocene values. However, the ice core data between 20 and 10 ka are sparse.

The planktonic $\delta^{13}C$ records (*23, 24, 26*) show that the $\delta^{13}C$ trough centered on termination I is about half of that centered on termination II (Fig. 4). The DH-11 record does not extend to termination I, however, so a direct comparison cannot be made with the plant (*28, 29*) and ice core (*30*) records. The portion of the 1.3-per-mil shift (across termination II) in the DH-11 core that is attributable to global change may be clarified when CO_2 in 160,000- to 110,000-year-old ice from Greenland or Antarctica is analyzed for $\delta^{13}C$.

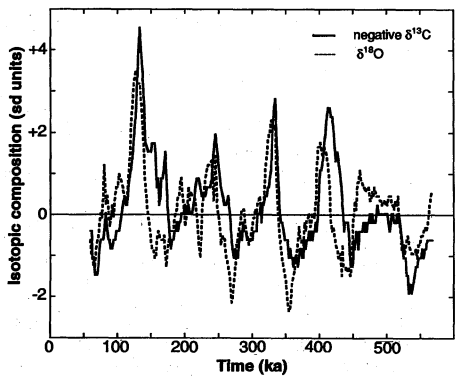

Fig. 3. Variation in $\delta^{13}C$ and $\delta^{18}O$ in core DH-11 in standard deviation units versus age. Curve for $\delta^{13}C$ is inverted. Age scale is same as in (*2*).

Might the $\delta^{13}C$ variations in the DH-11 core reflect changes in density and extent of vegetation in the recharge area? A primary source of carbon in the DIC of ground water is that generated in soils (*31*). The $\delta^{13}C$ of soil air varies inversely with vegetation density and extent (*31*). Declines in the DH-11 $\delta^{13}C$ profile (for example, from 355 to 335 ka in Fig. 2), which are coupled with ascending (warming) parts of the $\delta^{18}O$ curve, might therefore reflect increasing vegetation (and vice versa, as from 335 to 315 ka).

To address this hypothesis requires paleoecological—and related paleohydrologic and paleoclimatologic—data for the period 560 to 60 ka. Because such information is largely restricted to the past 30,000 years in the southern Great Basin, we assume that had the DH-11 $\delta^{13}C$ record extended to the Holocene, it would have shown (i) decreasing $\delta^{13}C$ values during the Wisconsinan deglaciation, (ii) a $\delta^{13}C$ minimum as peak interglacial temperature was achieved (at ~11 ka), and (iii) sharply increasing $\delta^{13}C$ values between ~11 ka and the present.

Studies of packrat middens have demonstrated that vegetation ecotones in the southern Great Basin shifted as much as 1000 m downward during the last full glacial climate in comparison to modern plant occurrences (*32*). At such times, when mean annual temperatures are believed to have been at least 6°C cooler (*33*) and mean annual precipitation was 30 to 40% greater (*34*), pygmy-conifer woodlands extended (Fig. 1) to altitudes as low as 900 m (versus above 2000 m today); subalpine conifer forests typified by limber pine (*Pinus flexilis*) grew at altitudes as much as 600 m lower in the Sheep Range (*33*). It is thus likely that during full glacial times the highest several hundred to 1000 m of the Spring Mountains—presumably the major source of recharge—had alpine rather than the denser subalpine vegetation present today. Conversely, from the end of full glacial (21 ka) to peak interglacial (~11 ka) climates, vegetation ecotones presumably expanded upward such that the density of the vegetation on the highest portions of the Spring Mountains was increased. In the Eleana Range (altitude 1800 m) limber pine, which is not a drought-tolerant plant, co-existed with steppe shrubs until at least 13.2 ka. By 11.7 ka this community was replaced by a drought-tolerant pinyon-juniper woodland. Concomitantly, pygmy-conifer woodland disappeared from all the intermediate altitude (<1800 m) ridges of the region (Fig. 1) by ~12 to ~10 ka, marking the end of a period of mesophytic vegetation.

Under the vegetative density hypothesis sparsest vegetation (in upland recharge areas) occurred during mid- to full glacial times (that is, ~390 to ~355, ~315 to ~275, ~200 to ~180, and ~100 to ~20 ka; Fig. 2). Declining $\delta^{13}C$ values in the DH-11 core during deglaciations reflect the gradual revegetation of the highest (and wettest) 600 to 1000 m of the Spring Mountains, an area that, by analogy with the Sheep Range (*33, 34*), likely had only alpine or sparse subalpine vegetation during full glacial climates. Densest vegetation was attained at the beginning of the last four interglacials at 414, 334, 246, and 133 ka. The sharp reversals and increase in $\delta^{13}C$ that began just after these times (Fig. 2) are taken to reflect a sudden and dramatic reduction in vegetative density or extent in response to high interglacial temperature and possibly changes in seasonality of precipitation (*35*). This hypothesized reduction in vegetation at the beginning of interglacials (several thousand years before a decrease in $\delta^{18}O$) may account for why the $\delta^{13}C$ time series leads the $\delta^{18}O$ time series. The $\delta^{13}C$ reversal may also reflect deforestation of the intermediate altitude ridges of the region [those less than 1800 m, for example, Desert, Pintwater, Spotted, and Specter ranges (Fig. 1)], provided such ridges contributed significantly to full glacial recharge. This deforestation was completed between ~12 and ~10 ka (*33*), and presumably at equivalent times in earlier glacial cycles. According to this hypothesis, the sharp $\delta^{13}C$ minimum at 133 ± 2 ka would indicate that the retreat of the North American ice sheets was essentially complete 5000 years before the exceptional high in Northern Hemisphere summer insolation at 128 ± 1 ka (*36*).

Decreasing $\delta^{13}C$ values during deglaciations may also be explained by glacial meltwater discharges into the Gulf of Mexico, which might have increased summer precipitation over the southwestern United States by strengthening the Bermuda high and shifting it westward (*37*). In addition, the sharp reversals in $\delta^{13}C$ (particularly at 334, 246, and 133 ka) might reflect (*38*,

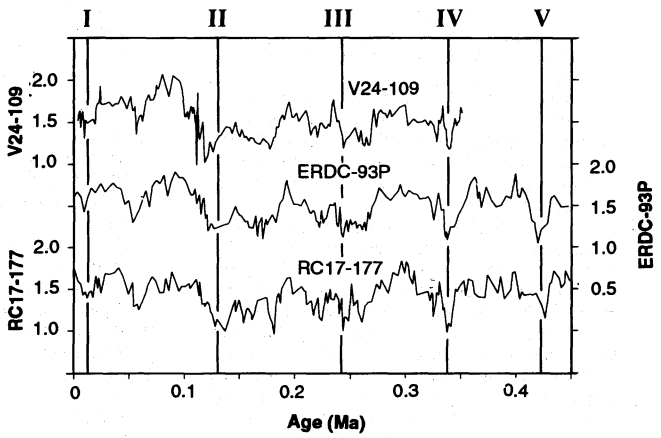

Fig. 4. Variation in $\delta^{13}C$ in planktonic foraminifera in three cores from non-upwelling, nutrient-poor portions of the western equatorial Pacific Ocean. Illustration from (*24*); vertical lines and Roman numerals have been added to show the location of SPECMAP (*2*) terminations V through I. Similar plots are published for cores from the west and east equatorial Atlantic (*26*) and from the southwestern Gulf of Mexico (*23*).

39) northward retreat of the southern branch of the jet stream.

The vegetative density hypothesis is seemingly contradicted by some paleohydrologic evidence. For example, between ~130 and 35 ka, Searles Lake contained fresh water (*40*), and between 120 and ~20 ka the water table in Browns Room stood 6 to 9 m above the modern level (*18*). Yet, during this time, the DH-11 $\delta^{13}C$ record increased by 1.3 per mil [its maximum shift in the last 500,000 years (Fig. 2)], indicative of declining vegetative density at a time of presumably high effective moisture. Conversely, between 15 to 20 ka and the present, the water table in Browns Room declined 9 m and Searles Lake desiccated (*18, 40*); this period includes an interval of anticipated decreasing $\delta^{13}C$ in the DH-11 core and, accordingly, increasing vegetation. We conclude that the DH-11 $\delta^{13}C$ record in the Ash Meadows basin is not an indicator of ground-water recharge or lake levels, but rather a record of extent and density of vegetation on a major upland. Other workers have also noted a lack of correspondence between effective moisture and vegetation (*33, 41*).

Vegetation density does not explain some features of the DH-11 $\delta^{13}C$ curve. Between ~180 and ~155 ka and between 450 and 435 ka (Fig. 2), the $\delta^{13}C$ curve declines about half way to its minimum value while the $\delta^{18}O$ curve fluctuates by only a few tenths of a per mil. Perhaps these periods reflect the gradual reforestation of recharge areas. The interval ~235 to ~220 ka is another puzzle in that the $\delta^{18}O$ curve declines 1 per mil to full glacial values (+13.6 per mil), while the $\delta^{13}C$ curve does not fluctuate.

In summary, the Devils Hole $\delta^{13}C$ record contains two major unresolved puzzles. Lack of obliteration of $\delta^{13}C$ variations during the 80 km aquifer-flow path to Devils Hole and arrival of the $\delta^{13}C$ signal before the conservative $\delta^{18}O$ tracer pose a hydrogeochemical conundrum. And, whether the $\delta^{13}C$ variations reflect changes in density of vegetation in local uplands, global changes in $\delta^{13}C$ of atmospheric CO_2, both factors, or as yet undetermined causes, constitutes a paleoclimatologic riddle.

REFERENCES AND NOTES

1. K. R. Ludwig, K. R. Simmons, B. J. Szabo, I. J. Winograd, A. C. Riggs, *Science* **258**, 284 (1992).
2. I. J. Winograd *et al.*, *ibid.*, p. 255.
3. I. J. Winograd, B. J. Szabo, T. B. Coplen, A. C. Riggs, *ibid.* **242**, 1275 (1988); R. J. Hoffman, *U.S. Geol. Surv. Open-File Rep. 88-93* (1988).
4. I. J. Winograd and W. Thordarson, *U.S. Geol. Surv. Prof. Pap. 712-C* (1975); W. W. Dudley Jr. and J. D. Larson, *ibid. 927* (1976).
5. I. J. Winograd and F. J. Pearson Jr., *Water Resour. Res.* **12**, 1125 (1976).
6. Vein-calcite samples analyzed include DH-2 (*3*), DH-7, DH-10, and DH-11, collected at depths below the water table of ~20 m, ~30 m, ~15 m, and ~31 m, respectively.
7. W. S. Broecker [*Nature* **359**, 779 (1992)] suggested that the relatively flat and lengthy (10,000- to 20,000-year) interglacial peaks in the DH-11 $\delta^{18}O$ curve may reflect mixing in the aquifer. However, the $\delta^{13}C$ curve shows a dramatic increase in ^{13}C content while the $\delta^{18}O$ curve remains relatively constant (Fig. 2). Peak interglacial $\delta^{18}O$ values of 10,000-year duration also occur in the marine record [M. Sarnthein and R. Tiedemann, *Paleoceanography* **5**, 1041 (1990)] for isotope substage 5e.
8. J. M. Landwehr *et al.*, *Geol. Soc. Am. Abstr. Prog.* **22**, 209 (1990).
9. Matrix diffusion can also lower ^{14}C content in DIC in carbonate aquifers, perhaps by a factor of 10 to 1000 in some chalk aquifers [P. Maloszewski and A. Zuber, *Water Resour. Res.* **27**, 1937 (1991)]. Additionally, in this tectonically active environment, fresh carbonate bedrock fracture surfaces are created continuously by ongoing tectonic extension (*10*).
10. W. J. Carr, *U.S. Geological Survey, Open File Rep. 87-560* (1988); A. C. Riggs, P. T. Kolesar, R. J. Hoffman, in preparation.
11. R. J. Ross, Jr., V. Jaanusson, I. Friedman, *U.S. Geol. Surv. Prof. Pap. 871* (1975); C. J. Boughton, thesis, University of Nevada, Reno (1986)].
12. K. Emrich, D. H. Ehhalt, and J. C. Vogel [*Earth Planet. Sci. Lett.* **8**, 363 (1970)] measured 0.035 ± 0.013 per mil/°C for the temperature dependence of the calcite-bicarbonate carbon isotope fractionation factor. We know from the DH-11 $\delta^{18}O$ studies (*2*) that Devils Hole temperature variation during the period of our record is negligible; however, even if the entire $\delta^{18}O$ shift (2.7 per mil) were attributed to temperature change, such a change (13.2°C) would only cause a 0.5-per mil change in $\delta^{13}C$. The water table in Devils Hole has fluctuated ~9 m in the past ~120,000 years (*18*). Yet, for a large range of depths below water table (~15 to ~31 m), the magnitude of $\delta^{13}C$ (and $\delta^{18}O$) variations in calcite vein specimens was identical (*6*), indicating that the $\delta^{13}C$ values are independent of water pressure.
13. To determine if modern calcite is precipitating in carbon isotopic equilibrium, we studied three samples of recent calcite (two samples were from coatings on a flash bulb floating in Devils Hole). The mean $\delta^{13}C$ was −1.75 ± 0.2 per mil. The $\delta^{13}C$ of DIC of ground water from Devils Hole is −4.8 ± 0.2 per mil (*5*). For a water temperature of 34°C, pH of 7.4, and alkalinity of 5.01 meq/liter, we calculate carbon speciation of 93% bicarbonate and 7% aqueous CO_2 and a carbon isotopic fractionation between modern calcite and dissolved bicarbonate of 2.39 per mil, within the range of laboratory and empirical measurements [M. Rubinson and R. N. Clayton, *Geochim. Cosmochim. Acta* **33**, 443 (1969); J. V. Turner, *ibid.* **46**, 1183 (1982)]. An additional factor supporting the likelihood of carbon isotopic equilibrium is that the average growth rate of the DH-11 core is slow (~0.7 mm per thousand years).
14. Expectable pH changes in the regional carbonate aquifer of a few tenths would probably influence $\delta^{13}C$ by less than 0.1 per mil. Even increasing the pH from its present value of 7.4 to the unreasonable value of 9—this is a carbonate-buffered system—only decreases $\delta^{13}C$ of calcite by 0.5 per mil [figure 3 of T. M. L. Wigley, L. N. Plummer, F. J. Pearson Jr., *Geochim. Cosmochim. Acta* **42**, 1117 (1978)].
15. We rule out local effects at Devils Hole—for instance, ephemeral input of surface water during convective summer storms—because (i) ground-water flows upward at Ash Meadows (*4*) and would dilute dramatically (and make unrecognizable) any short-lived surface-water input, and (ii) the chemical and stable isotopic composition of Devils Hole water is identical to water from the major artesian springs along the 16-km-long spring lineament at Ash Meadows (*5*); these springs discharge as much as 180 liter/s.
16. Varying the amount of ground-water underflow derived from Pahranagat Valley relative to the Spring Mountains or Sheep Range (Fig. 1) will not likely produce significant variations in $\delta^{13}C$ because the $\delta^{13}C$ values of these sources are similar [see (*5*)]. $\delta^{13}C$ of DIC at Devils Hole might also be affected by varying the fraction of carbon derived from downward leakage of water from Tertiary aquitards into the underlying regional carbonate aquifer. This source may contribute as much as 20% of the alkalinity measured at Ash Meadows (*4, 5*). However, the permeability of the aquitard is very low [3×10^{-7} to 3×10^{-9} cm/s (*4*)] and its thickness is hundreds of meters. Therefore, it is unlikely that variations in aquitard leakage could be responsible for the relatively rapid variations in the DH-11 $\delta^{13}C$ time series.
17. Increasing ground-water recharge rates will increase ground-water velocities and reduce the time for exchange between DIC and Paleozoic carbonate rock, which would presumably lead to more negative $\delta^{13}C$ values. By this mechanism, we would infer that past transitions from full glacial climate to peak interglacials were periods of increasing ground-water recharge. However, just the opposite has been observed during Termination I. On the basis of dating of speleothems in Browns Room, a subaerial room in Devils Hole cavern, B. Szabo and colleagues (*18*) found that the water table in Devils Hole remained relatively high throughout the period ~120 to 20 ka and that it declined 9 m in the last 20,000 years.
18. B. Szabo *et al.*, *Quat. Res.*, in press.
19. While the average growth rate of the DH-11 core was ~0.7 mm per 10^3 years, the rate actually varied between ~0.3 to ~1.3 mm per 10^3 years (*1*). That these variations cannot be responsible for the $\delta^{13}C$ variations is seen by focusing on the period 156 to 120 ka, for which we have the densest time control (*1*). From ~150 to ~122 ka the growth rate varied narrowly between ~0.3 and ~0.4 mm per 10^3 years, the lowest rates in our record. Yet, during this period, which straddles termination II, the $\delta^{13}C$ displays its most dramatic variations (Fig. 2). Conversely, between ~122 to ~120 ka, the highest indicated growth rate (~1.3 mm per 10^3 years) is not marked by any departure of the $\delta^{13}C$ curve from its orderly return toward full glacial baseline levels (Fig. 2).
20. Soil gas generated by C4 plants is enriched by as much as 10 per mil in $\delta^{13}C$ compared to that of plants utilizing other pathways [R. Park and S. Epstein, *Geochim. Cosmochim. Acta* **21**, 110 (1960); *Plant Physiol.* **36**, 133 (1961)]. However, between 2270 and 2740 m in the Spring Mountains (the major recharge area), Quade *et al.* (*21*) found that 100% of modern vegetation is composed of C3, not C4, plants. Presumably C3 plants also dominated the recharge area during earlier interglacials.
21. J. Quade, T. E. Cerling, J. R. Bowman, *Bull. Geol. Soc. Am.* **101**, 464 (1989).
22. J. M. Barnola, D. Raynaud, Y. S. Korotkevich, C. Lorius, *Nature* **329**, 408 (1985).
23. D. F. Williams, in *The Carbon Cycle and Atmospheric CO_2: Natural Variations Archean to Present*, E. T. Sundquist and W. S. Broecker, Eds. (*Geophys. Monogr. Ser. 32*, American Geophysical Union, Washington, DC, 1985), pp. 329–341.
24. N. J. Shackleton, J. Le, A. Mix, M. A. Hall, *Quat. Sci. Revs.* **11**, 387 (1992).
25. D. W. Oppo and R. G. Fairbanks, *Paleoceanography* **4**, 333 (1987).
26. W. B. Curry and T. J. Crowley, *ibid.* **2**, 489 (1987).
27. P. D. Quay, B. Tilbrook, C. S. Wong, *Science* **256**, 74 (1992).
28. R. V. Krishnamurthy and S. Epstein, *Tellus* **42B**, 423 (1990).
29. B. D. Marino, M. B. McElroy, R. J. Salawitch, W. G. Spaulding, *Nature* **357**, 461 (1992).
30. M. Leuenberger, U. Siegenthaler, C. C. Langway, *ibid.*, p. 488.
31. DIC in ground-water recharge in the Great Basin can originate from dissolution of nominally 1 part Paleozoic carbonate [$\delta^{13}C = \sim -1$ per mil, (*11*)] by 1 part soil CO_2 ($\delta^{13}C = -25$ per mil) in highly

vegetated areas or by 1 part atmospheric CO_2 ($\delta^{13}C = -7$ per mil) in arid regions with little or no vegetal covering [T. E. Cerling, *Earth Planet. Sci. Lett.* **71**, 229 (1984)]. Amundson *et al.* [R. G. Amundson, O. A. Chadwick, J. M. Sowers, H. E. Doner, *Quat. Res.* **29**, 245 (1988)] and Quade *et al.* (*21*) independently demonstrated that $\delta^{13}C$ of modern soil CO_2 in alluvial fans bordering the Spring Mountains decreases with increasing altitude (from 840 to 2740 m) and concomitant increasing plant density. Thus, the $\delta^{13}C$ of DIC can range from −13 to −4 per mil between regions of dense and no vegetation, respectively.

32. J. L. Betancourt, T. R. Van Devender, P. S. Martin, Eds., *Packrat Middens: The Last 40,000 Years of Biotic Change* (Univ. of Arizona Press, Tucson, 1990).
33. W. G. Spaulding, in (*32*), pp. 166–199.
34. ———, *U.S. Geol. Surv. Prof. Pap. 1329* (1985).
35. R. S. Thompson, in (*32*), pp. 200–239.
36. A. Berger and P. Pestiaux, in *Milankovitch and Climate*, A. Berger, J. Imbrie, J. Hays, G. Kukla, B. Saltzman, Eds. (Reidel, Boston, 1984), part 1, pp. 83–111; A. L. Berger, *Quat. Res.* **9**, 139 (1978).
37. K. A. Maasch and R. J. Oglesby, *Paleoceanography* **5**, 977 (1990).
38. S. Manabe and A. J. Broccoli, *J. Geophys. Res.* **90**, 2167 (1985).
39. J. E. Kutzbach and P. J. Guetter, *J. Atmos. Sci.* **43**, 1726 (1986).
40. J. L. Bischoff, R. J. Rosenbauer, G. I. Smith, *Science* **227**, 1222 (1985).
41. I. C. Prentice, J. Guiot, S. P. Harrison, *Nature* **360**, 658 (1992).
42. G. Hut, Consultants' Group Meeting on Stable Isotope Reference Samples for Geochemical and Hydrological Investigations, Vienna, 16 to 18 September 1985. Report to Director General, International Atomic Energy Agency, Vienna, 42 (1987).
43. We thank J. K. Böhlke, J. Thomas, E. Spiker, E. Sundquist, and T. E. Cerling for review comments; L. N. Plummer and F. J. Pearson Jr. for helpful discussions; and S. Andersen, J. Chen, J. Forsythe, C. Gwinn, and J. Hopple for excellent analytical aid.

2 August 1993; accepted 18 November 1993

Distinguishing the Direct and Indirect Products of a Gas-Surface Reaction

Charles T. Rettner and Daniel J. Auerbach

It has long been postulated that gas-surface chemical reactions can occur by means of two distinct mechanisms: direct reaction on a single gas-surface encounter or reaction between two adsorbed species. It is shown here that these mechanisms have distinct dynamical signatures, as illustrated by the reaction of hydrogen with chlorine on gold(111). The direct reaction product leaves the surface with a high kinetic energy in a narrow angular distribution that displays a "memory" of the direction and energy of the incident hydrogen atom. The indirect reaction product has a near-thermal energy distribution and an angular distribution that is close to that of a cosine function.

Gas-surface reactions are generally classified in terms of two idealized mechanisms (*1*). Some reactions are believed to occur more or less directly as a gas-phase reagent strikes an adsorbate, whereas other reactions are believed to involve reagents that are chemisorbed and in thermal equilibrium with the surface. We show that these two mechanisms can be distinguished by measuring the dynamical properties of the product. We illustrate this approach with results for the reaction of H with Cl on Au(111). We find that the direct reaction product leaves the surface with a high kinetic energy in a narrow angular distribution that displays a "memory" of the direction and energy of the incident H atom. In contrast, we find that the indirect reaction product has a near-thermal energy distribution and an angular distribution that is close to that of a cosine function.

The above-mentioned reaction mechanisms were proposed more than 70 years ago. Researchers at that time speculated that an impinging atom or molecule can react directly upon striking an adsorbed species in a process that is now referred to as an Eley-Rideal (ER) mechanism. These researchers believed that reactions can also occur between species that have become fully accommodated to the surface in a process that is now referred to as a Langmuir-Hinshelwood (LH) mechanism. Although these mechanisms are consistent with chemical intuition and with observations of reaction rates (*1–4*), there was no direct evidence to support them. Such proof has been slow in coming. In 1922, Irving Langmuir (*2*) stated that, "With our increasing knowledge of the structure of solid bodies and of the atoms and molecules of which they are built we should now . . . gradually begin to gain a clear insight into the mechanisms of surface reactions." But only recently have we begun to gain the expected insight into mechanisms of surface reactions. The reason is simple. In order to probe reaction mechanisms [and to make contact with detailed calculations (*5, 6*)], one must go beyond structural and kinetic measurements to measurements of the nascent distributions of reaction products with respect to angle (*7*), kinetic energy (*7, 8*), or internal state (*9–11*).

We have carried out such measurements for the reaction of H atoms with Cl adsorbed on a Au(111) surface. We show that the HCl product of this process is produced by both ER and LH mechanisms. Specifically, we have obtained information on the velocity and angular distributions of the HCl product. These measurements exhibit a clear bimodality that reflects the two mechanisms. Moreover, the HCl produced by the ER process has an angular distribution and a mean kinetic energy that depends on the kinetic energy of the incident H atom. Our results are consistent with a previous study of this system by Lykke and Kay (*11*). These researchers used laser ionization detection to determine the internal state distributions of the HCl product as a function of surface temperature. On the basis of their findings, Lykke and Kay were the first to suggest that this reaction might proceed by both ER and LH mechanisms. They were not, however, able to demonstrate correlations between initial state and final state properties, which are needed to prove that an ER mechanism applies.

The apparatus and techniques needed are similar to those used previously in studies of dissociation and inelastic scattering dynamics (*7, 12*). Beams of H atoms are chopped to produce short pulses and then directed at a Au(111) surface covered with a saturation layer of Cl (*13*). Two H atom beam sources are used. In one, the H_2 is dissociated by a microwave discharge in a quartz tube (*14*). This source gives H atoms with a mean kinetic energy of ~0.07 eV. The other source is based on thermal dissociation of H_2 in a graphite tube held at 2200 K (*15*). This source gives H atoms with a mean kinetic energy of ~0.3 eV. The angle of incidence of the H atoms is 60° from the surface normal in both cases. The Cl is supplied to the surface from a second beam

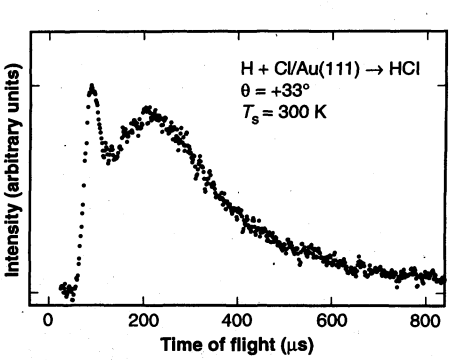

Fig. 1. Time-of-flight distribution of HCl formed by the reaction of H atoms with Cl/Au(111). This distribution was obtained for T_s = 300 K at a detection angle of 33° from the surface normal. The incident H atoms have a mean kinetic energy of 0.07 eV and an incidence angle of 60°.

IBM Research Division, Almaden Research Center, 650 Harry Road, San Jose, CA 95120.